

Transmural Left Ventricular Shear Strain Alterations Adjacent to and Remote from Infarcted Myocardium

Allen Cheng¹, Frank Langer¹, Tom C. Nguyen¹, Marcin Malinowski¹, Daniel B. Ennis², George T. Daughters^{1,3}, Neil B. Ingels, Jr.^{1,3}, D. Craig Miller¹

Departments of ¹Cardiovascular and Thoracic Surgery and ²Radiology, Stanford University School of Medicine, Stanford, and ³Laboratory of Cardiovascular Physiology and Biophysics, Research Institute of the Palo Alto Medical Foundation, Palo Alto, California, USA

Background and aim of the study: In some patients, dysfunction in a localized infarct region spreads throughout the left ventricle to aggravate mitral regurgitation and produce deleterious global left ventricular (LV) remodeling. Alterations in transmural strains could be a trigger for this process, as these changes can produce apoptosis and extracellular matrix disruption. The hypothesis was tested that localized infarction perturbs transmural strain patterns not only in adjacent regions but also at remote sites.

Methods: Transmural radiopaque beadsets were inserted surgically into the anterior basal and lateral equatorial LV walls of 25 sheep; additional markers were used to silhouette the left ventricle. One week thereafter, 10 sheep had posterior wall infarction from (obtuse marginal occlusion, INFARCT) and 15 had no infarction (SHAM). Four-dimensional marker dynamics were studied with biplane videofluoroscopy eight weeks later. Fractional area shrinkage, LV volumes and transmural circumferential, longitudinal and radial systolic strains were analyzed.

In some patients - particularly those exhibiting chronic ischemic mitral regurgitation - localized myocardial infarction leads to deleterious global left ventricular (LV) remodeling, which is characterized by a number of degenerative changes in cardiac structure and function (1-4). Further, infarct extension can initiate this global myopathic process (2,4-7). Regional dysfunction, initially localized within the infarcted

Results: Compared to SHAM, INFARCT greatly increased longitudinal-radial shear (midwall: 0.07 ± 0.07 versus 0.14 ± 0.06 ; subendocardium: 0.03 ± 0.07 versus 0.20 ± 0.08) in the inner half of the lateral LV wall and increased circumferential-radial shear (midwall: 0.03 ± 0.05 versus 0.10 ± 0.04 ; subepicardium: 0.02 ± 0.05 versus 0.12 ± 0.10) increased in the outer half of the LATERAL wall. In the ANTERIOR wall, INFARCT also increased longitudinal-radial shear (midwall: 0.01 ± 0.05 versus 0.12 ± 0.04 ; subendocardium: 0.04 ± 0.09 versus 0.25 ± 0.20) in the inner layers.

Conclusion: Increased transmural shear strains were found not only in an adjacent region, but also at a site remote from a localized infarction. This perturbation could trigger remodeling processes that promote the progression of ischemic cardiomyopathy. A better understanding of this process is important for the future development of surgical therapies to reverse destructive LV remodeling.

The Journal of Heart Valve Disease 2006;15:209-218

myocardium, extends to the remainder of the ventricle and transforms normally perfused myocardium into dysfunctional remodeled myocardium. Altered LV wall strains have been proposed as a cause of infarct extension (2,4), and abnormal strain patterns can result in the production of cytokines and reactive oxygen species (ROS), which in turn stimulate myocyte apoptosis (8-10) and extracellular matrix disruption (11-13). Progressive LV dilation and LV chamber shape change can also lead to more myocyte stretch (14-17). This subsequently catalyzes a positive feedback loop of dilatation and further exaggeration of wall stress, which ultimately leads to heart failure. This feedback loop of LV dilatation and chamber shape change lead to progressive papillary muscle displacement, leaflet tethering, and annular dilatation as seen in chronic ischemia mitral regurgitation (18-20). In an attempt to interrupt this vicious cycle, various surgical therapies aimed at

Presented at the Third Biennial Meeting of the Society for Heart Valve Disease, 17th-20th June 2005, Vancouver Convention and Exhibition Centre, Vancouver, Canada

Address for correspondence:
D. Craig Miller MD, Department of Cardiothoracic Surgery, Falk Cardiovascular Research Center, Stanford University School of Medicine, 300 Pasteur Drive, Stanford, California 94305-5247, USA
e-mail: dcm@stanford.edu

reducing wall stress/strain and normalizing LV shape have received considerable attention recently.

Recent data (21) from an open-chest ovine model have shown that transmural strain patterns adjacent to ischemic myocardium are perturbed acutely; however, precise direct three-dimensional (3-D) measurements of regional transmural LV wall strains in regions adjacent to and remote from an infarction in a closed-chest model are lacking. The aim of the present study was to test the hypothesis that myocardial infarction alters transmural strain patterns not only in adjacent regions but also at remote LV sites. This perturbation of myocardial transmural strain patterns could serve as important triggers for the remodeling processes that promote progression from localized infarction to global ischemic cardiomyopathy. A better understanding of these alterations is important for the future design of surgical treatments to prevent or reverse LV remodeling in ischemic cardiomyopathy.

Materials and methods

Animals

Twenty-five adult Dorsett-hybrid sheep were used in these studies. All animals received humane care in compliance with the *Principles of Laboratory Animal Care* formulated by the National Society for Medical Research and the *Guide for Care and Use of Laboratory Animals* prepared by the National Academy of Sciences and published by the National Institutes of Health (DHEW NIHG publication 85-23, revised 1985). This study was approved by the Stanford Medical Center Laboratory Research Animal Review Committee and conducted according to Stanford University policy.

Surgical preparation and marker data acquisition

These surgical preparation and marker data acquisition methods have been described in detail previously (22,23), and therefore are only outlined here. Through a left thoracotomy, 25 sheep had 13 subepicardial radiopaque markers surgically implanted to silhouette the LV chamber (Fig. 1). Epicardial echocardiography was used to locate and measure the wall depth of the mid-lateral equatorial LV wall between the papillary muscles and a site in the anterior LV wall basal to the anterior papillary muscle. Three transmural columns of beads (four beads in each column; Fig. 1) were implanted into these two regions using a bead insertion trochar oriented normal to the regional epicardial tangent plane. The sheep were subdivided into SHAM ($n = 15$) and INFARCT groups ($n = 10$). In INFARCT animals, 2-0 polypropylene sutures were passed around one or two obtuse marginal branches of the left circumflex coronary artery located between the posterior vein of the left ventricle and the middle cardiac

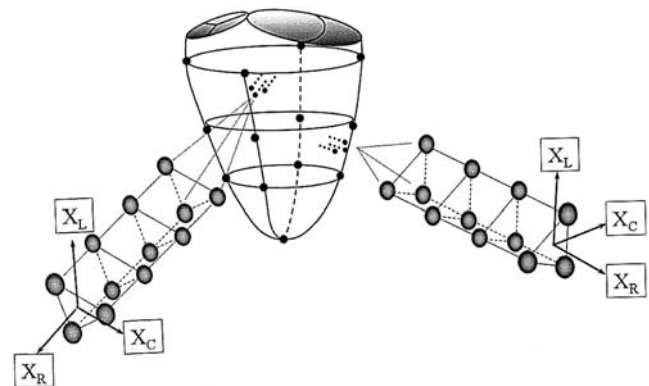


Figure 1: Locations of left ventricular (LV) epicardial markers and LV lateral equatorial and anterior basal wall transmural beadsets. X_C , X_L and X_R are the local circumferential, longitudinal and radial axes, respectively.

vein and loosely snared using the method of Llaneras et al. (24).

At one week postoperatively, the animals were taken to the cardiac catheterization laboratory, sedated with ketamine (25 mg/kg, i.m.), intubated, mechanically ventilated, and anesthesia maintained with inhalational isoflurane (1-2.5%). With the heart in normal sinus rhythm and ventilation arrested at end-expiration, simultaneous biplane videofluoroscopy (60 Hz), electrocardiogram and LV and aortic pressures were recorded during steady-state baseline conditions. Data from the two radiographic views were later digitized and merged to yield 3-D coordinates for each radiopaque marker every 16.7 ms. Immediately after baseline data were obtained, the INFARCT animals were premedicated with lidocaine (100 mg i.v.), bretylium (75 mg i.v.) and magnesium (3 g i.v.); the coronary artery snares were then tightened, producing complete occlusion of the selected vessels as verified angiographically (Fig. 2). Ventricular tachyarrhythmias were treated with lidocaine (50-100 mg i.v.) and bretylium (75-150 mg i.v.), as needed. The animals were then stabilized and subsequently recovered.

At eight weeks postoperatively, each animal was returned to the cardiac catheterization laboratory for the recording of hemodynamic and marker data. At the conclusion of the study, 3.0-mm perfusion coronary angioplasty balloon catheters (GUIDANT; AguilTrac Peripheral Catheter, Santa Clara, CA, USA) were placed into the proximal circumflex and left anterior descending coronary arteries. The animals were then euthanized by administration of sodium pentothal (1 g i.v.) followed by an intravenous bolus of potassium chloride (80 mEq.) to arrest the hearts at end-diastole. After adjusting LV pressure by blood withdrawal to match previous in-vivo LV end-diastolic pressure, 5%

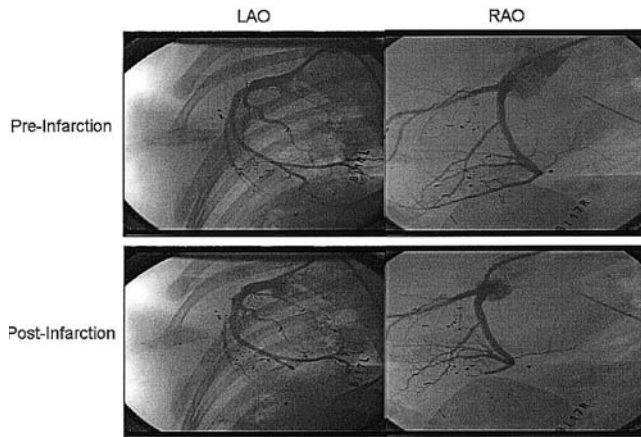


Figure 2: Coronary artery angiogram (left and right oblique biplane videofluoroscopic views). Coronary artery snares were tightened one week postoperatively to occlude OM2/OM3 to induce posterior wall infarction in the INFARCT group. Complete occlusion of the selected vessels was verified angiographically. OM2 was occluded in this representative animal (lower row).

buffered glutaraldehyde (300 ml) was infused through both coronary catheters simultaneously with the balloons inflated to fix the hearts in situ. The hearts were then explanted and stored in 10% formalin for histological examination.

Hemodynamics and cardiac cycle timing

Three consecutive steady-state beats in sinus rhythm were selected for analysis from each study. For each cardiac cycle, end-diastole (ED) was defined as the videofluoroscopic frame immediately prior to the upstroke of the LV pressure curve, defined by LV $dP/dt > 120$ mmHg/s. End-systole (ES) was defined as the videofluoroscopic frame when LV dP^2/dt^2 changed sign from minus to plus, a definition which captures the onset of relaxation and is consistent with the concept of end-systolic elastance. Instantaneous left ventricular volume (LVV) was calculated every 16.7 ms from the 3-D coordinates of the epicardial LV markers (Fig. 1) by summing the volumes of multiple space-filling tetrahedra.

Regional LV systolic function

Ventricular systolic fractional area shortening (FAS)

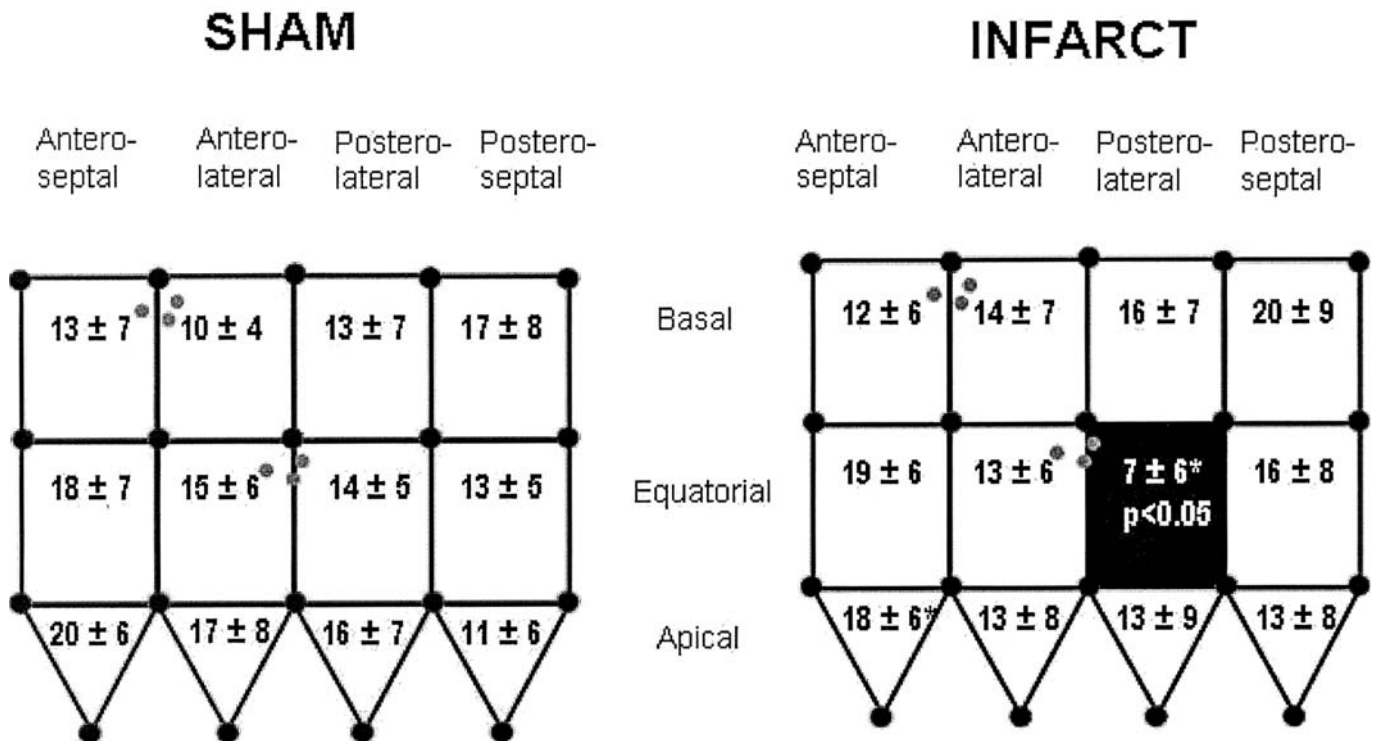


Figure 3: Systolic fractional area shortening (FAS) depicted as 3-D global LV marker array unrolled and projected onto a two-dimensional surface. Twelve contiguous LV epicardial regions (four basal, four equatorial, four apical regions) were defined and divided into antero-septal, anterolateral, posterolateral and posteroseptal walls. Calculated values for systolic FAS are shown for the SHAM (left panel) and INFARCT (right panel) groups. The gray area indicates the region with decreased FAS in the INFARCT group compared to SHAM. The two beadsets used to measure transmural strains are shown in gray circles. Note that the lateral equatorial beadset was adjacent to the infarcted myocardium while the anterior basal beadset was remote. Data shown are mean \pm SD. * $p < 0.05$ SHAM versus INFARCT.

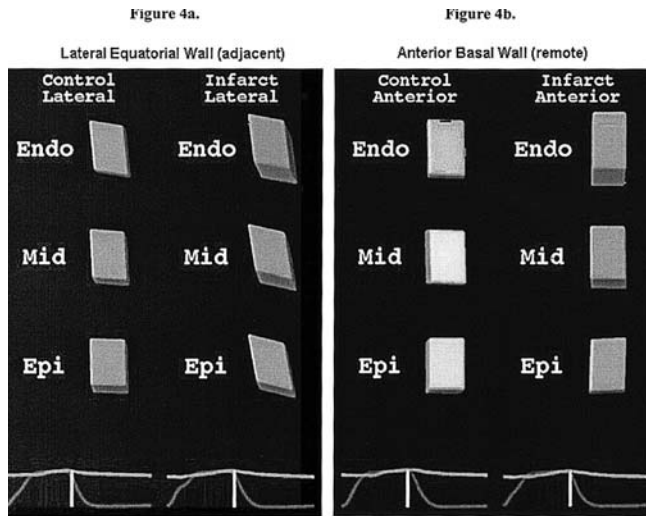


Figure 4: Three-dimensional transmural myocardial deformation animation throughout the cardiac cycle. Left: Summary of transmural cardiac strains of the lateral equatorial wall (adjacent to the infarct in the INFARCT group) at end-systole (ES) along the longitudinal (X_L), circumferential (X_C) and radial (X_R) axis. Right: The transmural cardiac strains of the anterior basal wall (remote from the infarct in the INFARCT group) at ES along the longitudinal (X_L), circumferential (X_C) and radial (X_R) axis. Note that the posterior wall infarction increased longitudinal-radial shear strain (in the midwall and endocardium) and circumferential-radial (in the midwall and epicardium) in the lateral wall of the INFARCT group (a). Infarction also increased longitudinal-radial strain in the anterior wall of the INFARCT group (b). See online archives (video 4a and 4b) for video clip demonstrating transmural deformations throughout the cardiac cycle.

was used as an index of regional LV systolic function to determine the functional demarcation between infarcted and non-infarcted myocardium. Each LV region defined by four subepicardial markers (Fig. 1) was divided into two triangular areas, and regional area was computed as the sum of these areas (Fig. 3). The apical region area was defined by a single triangle (Fig. 3). For each region, fractional change in systolic epicardial area (FAS) was computed as:

$$FAS = 100\% \times ([rArea_{ED} - rArea_{ES}] / rArea_{ED})$$
 where $rArea_{ED}$ was the regional area at ED and $rArea_{ES}$ the regional area at ES.

Finite cardiac strains

Placement of the transmural beadsets allowed assessment of transmural 3-D myocardial deformations in the lateral equatorial and anterior basal regions of the LV wall. The strain analysis methodology has been described in detail previously (22). Strains were reported at 20%, 50% and 80% depths from the epicardium, with ED as the reference configuration and ES as the deformed configuration.

Statistical analysis

Data were reported as mean \pm SD. All data were compared using two-way repeated measures ANOVA with Holm-Sidak pairwise multiple comparisons (Sigmastat 3.11; SPSS, Inc., Chicago, IL, USA) unless specified. A p-value <0.05 was considered to be statistically significant.

Results

All comparisons between the INFARCT and SHAM

Table I: Hemodynamic data for the two animal groups.

Parameter	SHAM (n = 15)		INFARCT (n = 10)	
	Baseline	8 weeks	Baseline	8 weeks
Heart rate (bpm)	104 \pm 16	104 \pm 20	98 \pm 13	96 \pm 22
LV dP/dt _{max} (mmHg/s)	1,660 \pm 385	1,533 \pm 438	1,496 \pm 255	1,534 \pm 259
EDV (ml)	102 \pm 17	105 \pm 27	113 \pm 34	137 \pm 49*
ESV (ml)	83 \pm 13	82 \pm 21	90 \pm 27	102 \pm 31*
SV (ml)	23 \pm 6	27 \pm 9	27 \pm 9	39 \pm 18*
EDP (mmHg)	11 \pm 6	7 \pm 8	13 \pm 5	10 \pm 5
ESP (mmHg)	101 \pm 18	106 \pm 14	101 \pm 12	111 \pm 25
LVP _{max} (mmHg)	104 \pm 19	111 \pm 14	102 \pm 12	115 \pm 25

Group mean (\pm SD) data from 25 hearts. p-values from two-sided paired-*t* test of eight-week data compared to baseline (one week post-op) data.

EDP: LV end-diastolic pressure; EDV: LV end-diastolic volume; ESP: LV end-systolic pressure; ESV: LV end-systolic volume; LV dP/dt_{max}: Maximum time derivative of LV pressure (LVP) during isovolumic contraction; LVP_{max}: LV maximum pressure; SV: Stroke volume.

*p <0.05 baseline versus eight weeks within the same group (Student's two-tailed paired *t*-test).

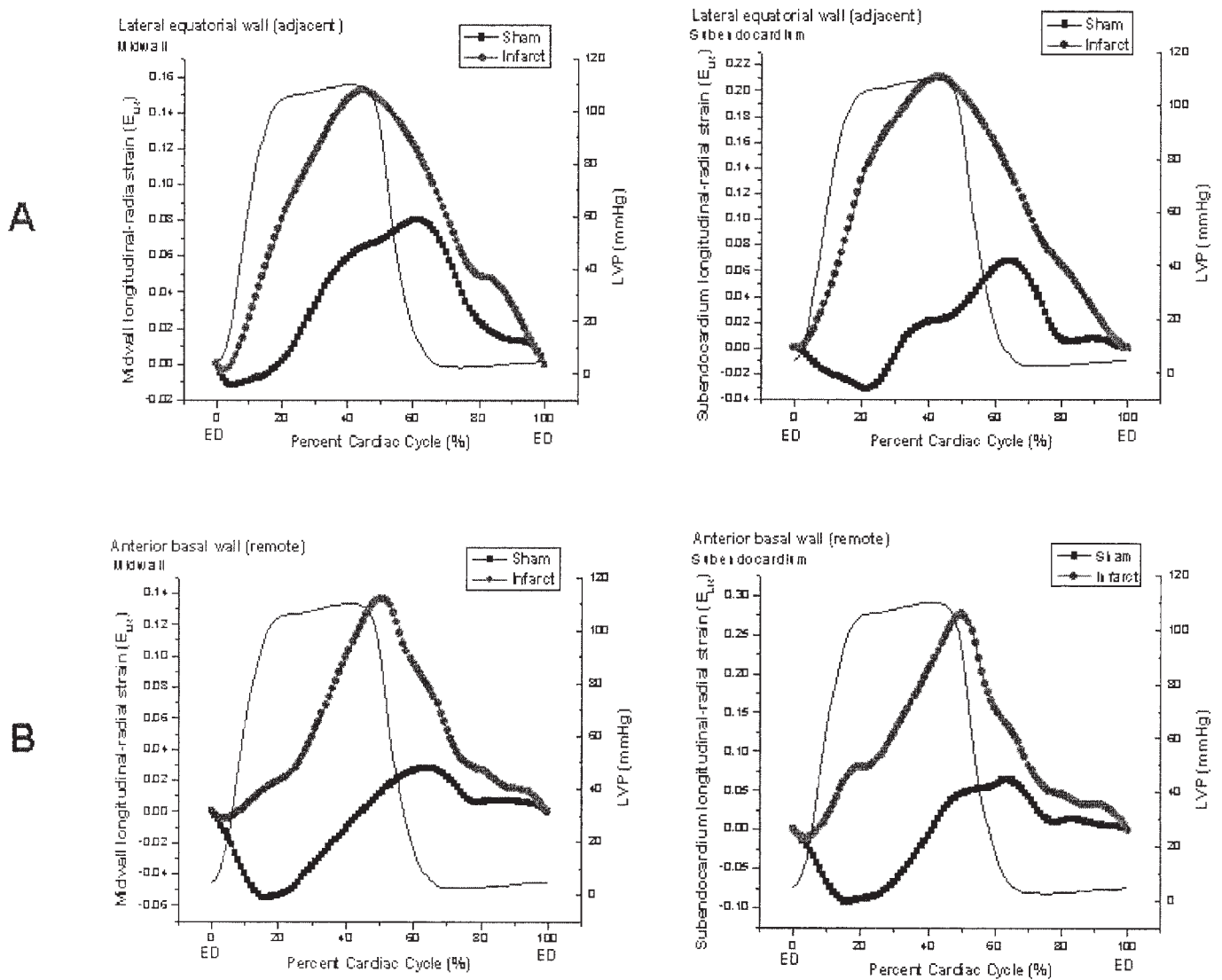


Figure 5: A) Plot of LV pressure (LVP) with simultaneous lateral LV wall longitudinal-radial shear strain in the midwall and subendocardial layers versus time of the cardiac cycle for the SHAM and INFARCT groups. B) Similar plot of LVP and LV longitudinal-radial shear strain in the midwall and subendocardium for the anterior basal LV region.

groups were based on the eight-week data. Hemodynamic data for both groups (SHAM and INFARCT) are summarized in Table I. The left ventricle dilated (i.e. both end-diastolic volume and end-systolic volume became larger) over the seven-week observation period in INFARCT animals, while heart size in the SHAM animals was unchanged. Stroke volume increased at eight weeks in the INFARCT group. No other hemodynamic parameters changed significantly between the baseline and eight-week studies in both groups. The fact that LV end-diastolic pressure did not become elevated after infarction in the INFARCT group reflected indirectly that these animals were not in congestive failure.

The group mean FAS in the SHAM and INFARCT animals is summarized in Figure 3. Consistent with occlusion of the targeted obtuse marginal branches, infarction decreased systolic FAS in the posterolateral equatorial region in the INFARCT group (Fig. 3; gray region), adjacent to the lateral equatorial beadset; as also illustrated in Figure 3, the anterior basal beadset was remote from the infarct.

Transmural systolic cardiac strains (group mean) at eight weeks in the lateral equatorial LV wall are shown in Table II (ED reference configuration; ES deformed configuration). Compared to SHAM, INFARCT exhibited greater longitudinal-radial shear strain (E_{LR}) in the inner half and circumferential-radial shear (E_{CR}) in the

subepicardium and midwall of the lateral wall adjacent to the infarct. No other cardiac strain differed significantly between SHAM and INFARCT.

Group mean transmural systolic cardiac strains in the anterior basal LV wall, remote from the infarct, are listed in Table III. Relative to SHAM, the INFARCT group exhibited greater longitudinal-radial shear strain (E_{LR}) in the midwall and subendocardium. All other cardiac strains were not significantly different between SHAM and INFARCT.

Figure 4 depicts still frames from an animation illustrating total 3-D transmural myocardial deformation at three wall depths in both regions for the SHAM and INFARCT groups (see online archives (video 4a and 4b) for video clip demonstrating deformations throughout the cardiac cycle). Each glyph in Figure 4 illustrates how a perfect cube of tissue from each depth

at ED becomes deformed in all axes at ES. These still frames illustrate the increase in longitudinal-radial shear in the inner wall and circumferential-radial shear in the outer wall of the lateral equatorial region (Fig. 4a), as well as the increase in longitudinal-radial shear of the inner wall of the anterior basal region (Fig. 4b).

Figure 5 illustrates group mean longitudinal-radial shear strains (E_{LR}) throughout the cardiac cycle in the anterior basal and lateral equatorial LV regions for the two groups. INFARCT exhibited greater E_{LR} shear strains throughout the cardiac cycle (ED to ED) relative to SHAM in the midwall and endocardium in the lateral equatorial wall adjacent to the infarct. Longitudinal-radial shear also increased in the INFARCT group throughout the cardiac cycle in the inner wall of the anterior basal region, remote from the infarct.

Table II: Transmural lateral equatorial left ventricular (LV) wall systolic cardiac strains.

Parameter	SHAM (n = 10)	INFARCT (n = 9)
20% depth		
E_{CC}	-0.08 ± 0.04	-0.04 ± 0.08
E_{LL}	-0.01 ± 0.07	-0.01 ± 0.09
E_{RR}	0.17 ± 0.08	0.20 ± 0.16
E_{CL}	0.02 ± 0.02	0.04 ± 0.05
E_{LR}	0.10 ± 0.08	0.10 ± 0.09*
E_{CR}	0.02 ± 0.05	0.12 ± 0.10*
50% depth		
E_{CC}	-0.10 ± 0.05	-0.04 ± 0.09
E_{LL}	-0.02 ± 0.07	-0.02 ± 0.11
E_{RR}	0.17 ± 0.07	0.18 ± 0.10
E_{CL}	0.02 ± 0.03	0.05 ± 0.05
E_{LR}	0.07 ± 0.07	0.14 ± 0.06*
E_{CR}	0.03 ± 0.05	0.10 ± 0.04*
80% depth		
E_{CC}	-0.11 ± 0.08	-0.07 ± 0.08
E_{LL}	-0.05 ± 0.07	-0.03 ± 0.12
E_{RR}	0.20 ± 0.11	0.23 ± 0.20
E_{CL}	0.02 ± 0.03	0.07 ± 0.05
E_{LR}	0.03 ± 0.07	0.20 ± 0.08*
E_{CR}	0.06 ± 0.07	0.10 ± 0.12

Group mean (± SD) data. ED: Reference configuration; ES: Deformed configuration.

*p < 0.05 SHAM versus INFARCT within the same wall depth from two-way repeated measures ANOVA with Holm-Sidak pairwise multiple comparisons. Depth measured as a percentage of the radial distance from the epicardial bead to the most subendocardial bead.

E_{CC} : Circumferential strain; E_{CL} : Circumferential-longitudinal shear; E_{CR} : Circumferential-radial shear; E_{LL} : Longitudinal strain; E_{LR} : Longitudinal-radial shear; E_{RR} : Radial strain.

Table III: Transmural anterior basal left ventricular (LV) wall systolic cardiac strains.

Parameter	SHAM (n = 7)	INFARCT (n = 6)
20% depth		
E_{CC}	-0.07 ± 0.05	-0.07 ± 0.05
E_{LL}	-0.07 ± 0.08	-0.12 ± 0.07
E_{RR}	0.34 ± 0.26	0.33 ± 0.14
E_{CL}	-0.05 ± 0.04	-0.01 ± 0.02
E_{LR}	0.04 ± 0.07	0.03 ± 0.09
E_{CR}	0.00 ± 0.05	-0.01 ± 0.11
50% depth		
E_{CC}	-0.07 ± 0.08	-0.09 ± 0.04
E_{LL}	-0.08 ± 0.08	-0.08 ± 0.10
E_{RR}	0.37 ± 0.17	0.34 ± 0.18
E_{CL}	-0.06 ± 0.06	0.00 ± 0.03
E_{LR}	0.01 ± 0.05	0.12 ± 0.04*
E_{CR}	0.02 ± 0.15	0.01 ± 0.10
80% depth		
E_{CC}	-0.06 ± 0.08	-0.12 ± 0.07
E_{LL}	-0.12 ± 0.05	-0.05 ± 0.18
E_{RR}	0.47 ± 0.20	0.48 ± 0.40
E_{CL}	-0.02 ± 0.06	-0.03 ± 0.09
E_{LR}	0.04 ± 0.09	0.25 ± 0.20*
E_{CR}	0.01 ± 0.23	0.00 ± 0.18

Group mean (± SD) data. ED: Reference configuration; ES: Deformed configuration.

*p < 0.05 SHAM versus INFARCT within the same wall depth from two-way repeated measures ANOVA with Holm-Sidak pairwise multiple comparisons. Depth measured as a percentage of the radial distance from the epicardial bead to the most subendocardial bead.

Other abbreviations as Table II.

Discussion

Ventricular remodeling after myocardial infarction is manifested by changes in LV size, shape, structure and function. These geometric and functional alterations are associated with gene expression, cellular and interstitial changes (1,2,8,10-12,25,26). Infarct extension has been shown to be an important initiating event of this myopathic process and has been postulated to explain the progression from localized myocardial infarction to global ischemic cardiomyopathy (2,4-7). Regional dysfunction, initially localized within the infarcted myocardium, spreads to involve the remainder of the ventricle and converts normally perfused myocardium into remodeled, hypokinetic myocardium (2,4). The cause of infarct extension is not well established, but it has been proposed that it is caused by increased wall stress/strain adjacent to the infarcted region; an acute increase in transmural shear strain adjacent to the ischemic region (21) has recently been demonstrated. Altered transmural wall strain patterns have been associated with the production of cytokines and ROS, which in turn stimulate myocyte apoptosis, disruption of extracellular matrix secondary to activation of matrix metalloproteinases, and fibrosis (8,10-12,26). This cascade may cause subsequent collagen degradation and fibrosis that contribute to thinning and stretching of the infarct border zone, or infarct extension (2,4-7). Subsequently, the heart enters into a positive feedback loop of dilatation and further exaggerated wall stress, which ultimately leads to progressive global and regional dysfunction and heart failure. The present experiment allowed an examination to be made of the changes in transmural strains in myocardium adjacent to and remote from the infarcted region, that may be involved in such a biochemical cascade leading to infarct extension and LV remodeling. An understanding of this mechanical alteration could be important in the design of future surgical therapy (e.g., passive ventricular constraint, surgical anterior ventricular remodeling procedures (27,28), Pacing, Dor operation, Coapsys[®]) to arrest or even potentially to reverse LV remodeling.

The principal findings of the present study were that posterior wall infarction not only increased longitudinal-radial shear and circumferential-radial shear strain in the myocardium adjacent to the infarct, but also increased longitudinal-radial shear strain in regions remote from the infarct.

Rodriguez et al. (21), in an acute open-chest experiment from the present authors' laboratory, demonstrated an acute increase in circumferential-radial and longitudinal-radial shear adjacent to the ischemic myocardium during mid-circumflex coronary occlusion. The present study extended these investigations

to examine transmural strains in a chronic closed-chest preparation in regions both adjacent to and remote from the infarct. The results of both studies showed that infarction or ischemia increased circumferential-radial shear in the outer wall and longitudinal-radial shear in the midwall adjacent to the infarct. In the chronic INFARCT group, longitudinal-radial shear also increased in the subendocardium in this adjacent region. Both the acute ischemia preparation and the present chronic infarct experiment demonstrated the same positive increase in circumferential-radial and longitudinal-radial shears. These shear perturbations reflect the direct interaction between infarcted and non-infarcted myocardium, which could trigger infarct extension.

The addition of a second beadset in the present study allowed transmural strain patterns to be examined in myocardium remote from the infarcted region. Changes in shear strain were seen in the remote anterior basal wall; infarction increased longitudinal-radial shear in the midwall and subendocardium at the remote site. It is speculated that this could be a factor in the evolution from a localized myocardial infarction to a global ventricular disease, although the animals in the present study were only eight weeks postinfarction and not in heart failure.

Surgical therapies designed to inhibit infarct extension by reducing wall stress have received considerable recent attention. For example, passive epicardial LV constraint recently was proposed to prevent infarct extension and LV remodeling. Kelley et al. (29), using an ovine LV aneurysm model, stiffened the region by placing a tailored piece of Marlex mesh over the anticipated myocardial infarct. In mesh-stiffened animals, hemodynamics, stroke work and end-systolic elastance returned to preinfarction values by one week after infarction. The patch placed over the infarct area prevented infarct extension by increasing the collagen content and decreasing matrix metalloproteinase (MMP)-1 and MMP-2 activity in the border zone (13). Using a similar protocol, Moainie et al. (30) used Marlex mesh prophylactically to cover a posterior wall infarction. When compared to the uncovered infarct group, geometric analysis using multiple piezoelectric crystals indicated significantly less short-axis strain in the infarcted myocardium in the mesh-restrained hearts.

Passive ventricular constraint, such as the Acorn cardiac support device (CSD) has also received considerable attention, and may prevent infarct extension by providing external ventricular support to reduce myocardial stretch. Recent data from the Acorn Corcap[™] randomized clinical trial (31,32) were promising. Acker et al. (31) showed that a CSD added to mitral annuloplasty or replacement in patients with

non-ischemic cardiomyopathy and functional mitral regurgitation normalized LV size and shape over time, improved the patients' quality of life, and enhanced freedom from requiring another major cardiac procedure. Laboratory data also demonstrated that Acorn CSD can reverse LV remodeling: Pilla et al. (33) showed that a CSD reduces infarct area and improves myocardial energetics and LV ejection fraction in an experimental model of ischemic cardiomyopathy. Sabbah and colleagues reported that a CSD lowers stretch protein level, improves calcium cycling, and attenuates pro-apoptotic signaling in cardiomyocytes (34).

In summary, localized posterior infarction increased transmural shear strains (i.e., longitudinal-radial and circumferential-radial shear) not only in myocardium adjacent to but also in a site remote from the infarct. This remote shear strain perturbation could trigger remodeling processes that promote infarct extension in global LV remodeling. A better understanding of these strain patterns might be important for the future development of surgical therapies to prevent infarct extension and to reverse deleterious LV remodeling. Surgical strategies designed to reverse shear strain (both directional and magnitude) potentially may provide a new paradigm to prevent progression of localized myocardial infarction to global LV dysfunction by arresting the infarct extension process.

Study limitations

Considerable caution must be employed in applying the results from the present experiment in sheep to the clinical scenario in humans. The need for immediate glutaraldehyde fixation for quantitative histological microstructural measurement precluded the assessment of perfusion in the infarct region using dye or microsphere injection; instead, coronary angiography was used to confirm obtuse marginal artery occlusion, and FAS was calculated to define regional systolic function. A deeper understanding of myofiber and sheet structure myocardial dynamics is currently being explored in the present authors' laboratory using newly developed histological measuring techniques and transmural fiber-sheet strain analytical methods (35).

Significant shear strain perturbations were demonstrated, not only adjacent to but also remote from, the infarct. Although no molecular nor biochemical data were measured, these findings emphasize the need for further research regarding the cellular remodeling processes triggered by mechanical strain alterations, which might be important in the evolution into global ischemic cardiomyopathy. Potential concern exists regarding the effects of tissue injury on measured strains caused by the insertion of the radiopaque bead-

sets. Inert material (i.e., gold) was used for the beads; furthermore, heart wall mechanical measurements, using the current method, were similar compared to other those obtained with non-invasive methods (19).

Acknowledgements

The authors appreciate the superb technical assistance provided by Mary K. Zasio, Maggie Brophy and Katha Gazda. They also thank Drs. James W. Covell, Andrew D. McCulloch and Jeffrey H. Omens at the University of California, San Diego, and Dr. John C. Criscione at the Texas A&M University for their expertise, and generous help and advice. These studies were supported by grants HL-29589 and HL-67025 from the National Heart, Lung and Blood Institute. Drs. Cheng, Langer and Nguyen were Carl and Leah McConnell Cardiovascular Surgical Research Fellows. Drs. Cheng and Nguyen were recipients of the Thoracic Society Foundation Research Fellowship Award. Dr. Langer was also supported by the Deutsche Akademie der Naturforscher Leopoldina, Halle, Germany.

References

1. Pfeffer MA, Braunwald E. Ventricular remodeling after myocardial-infarction: Experimental observations and clinical implications. *Circulation* 1990;81:1161-1172
2. Ratcliffe MB. Non-ischemic infarct extension: A new type of infarct enlargement and a potential therapeutic target. *J Am Coll Cardiol* 2002;40:1168-1171
3. Moulton MJ, Downing SW, Creswell LL, et al. Mechanical dysfunction in the border zone of an ovine model of left-ventricular aneurysm. *Ann Thorac Surg* 1995;60:986-998
4. Jackson BM, Gorman JH, Moainie SL, et al. Extension of borderzone myocardium in postinfarction dilated cardiomyopathy. *J Am Coll Cardiol* 2002;40:1160-1167
5. Narula J, Dawson MS, Singh BK, et al. AE. Noninvasive characterization of stunned, hibernating, remodeled and nonviable myocardium in ischemic cardiomyopathy. *J Am Coll Cardiol* 2000;36:1913-1919
6. Jeremy RW, Hackworthy RA, Kelly DT, Harris PJ. Left-ventricular dilatation after infarction. *Circulation* 1984;70:309
7. Erlebacher JA, Weiss JL, Weisfeldt ML, Bulkley BH. Early dilation of the infarcted segment in acute transmural myocardial infarction: Role of infarct expansion in acute left ventricular enlargement. *J Am Coll Cardiol* 1984;4:201-208
8. Kang PM, Izumo S. Apoptosis and heart failure: A critical review of the literature. *Circ Res*

- 2000;86:1107-1113
9. Saraste A, Pulkki K, Kallajoki M, Henriksen K, Parvinen M, Voipio-Pulkki LM. Apoptosis in human acute myocardial infarction. *Circulation* 1997;95:320-323
 10. Olivetti G, Abbi R, Quaini F, et al. Apoptosis in the failing human heart. *N Engl J Med* 1997;336:1131-1141
 11. Tyagi SC, Lewis K, Pikes D, et al. Stretch-induced membrane type matrix metalloproteinase and tissue plasminogen activator in cardiac fibroblast cells. *J Cell Physiol* 1998;176:374-382
 12. Wilson EM, Moainie SL, Baskin JM, et al. Region and species specific induction of matrix metalloproteinases occurs with post myocardial infarction remodeling. *Circulation* 2002;106:345
 13. Bowen FW, Jones SC, Narula N, et al. Restraining acute infarct expansion decreases collagenase activity in borderzone myocardium. *Ann Thorac Surg* 2001;72:1950-1956
 14. Sadoshima J, Izumo S. Mechanical stretch rapidly activates multiple signal transduction pathways in cardiac myocytes: Potential involvement of an autocrine paracrine mechanism. *EMBO J* 1993;12:1681-1692
 15. Sadoshima J, Izumo S. Mechanotransduction in stretch-induced hypertrophy of cardiac myocytes. *J Receptor Res* 1993;13:777-794
 16. Sadoshima J, Izumo S. Signal transduction pathways of stretch-induced hypertrophy in neonatal rat cardiac myocytes in vitro. *Circulation* 1992;86:95
 17. Sadoshima J, Jahn L, Takahashi T, Kulik TJ, Izumo S. Molecular characterization of the stretch-induced adaptation of cultured cardiac cells: An in-vitro model of load-induced cardiac hypertrophy. *J Biol Chem* 1992;267:10551-10560
 18. Tibayan FA, Rodriguez F, Langer F, et al. Annular remodeling in chronic ischemic mitral regurgitation: Ring selection implications. *Ann Thorac Surg* 2003;76:1549-1554;discussion 1554-1555
 19. Tibayan FA, Rodriguez F, Zasio MK, et al. Geometric distortions of the mitral valvular-ventricular complex in chronic ischemic mitral regurgitation. *Circulation* 2003;108(Suppl.II):II116-II121
 20. Tibayan FA, Rodriguez F, Zasio MK, et al. Alterations in left ventricular curvature and principal strains in dilated cardiomyopathy with functional mitral regurgitation. *J Heart Valve Dis* 2003;12:292-299
 21. Rodriguez F, Langer F, Harrington KB, et al. Alterations in transmural strains adjacent to ischemic myocardium during acute midcircumflex occlusion. *J Thorac Cardiovasc Surg* 2005;129:791-803
 22. Cheng A, Langer F, Rodriguez F, et al. Transmural cardiac strains in the lateral wall of the ovine left ventricle. *Am J Physiol Heart Circulat Physiol* 2005;288:H1546-H1556
 23. Cheng A, Langer F, Malinowski M, et al. Transmural shear strains alteration adjacent to and remote from infarcted myocardium. Third Biennial Meeting of The Society of Heart Valve Disease, Vancouver, 2005.
 24. Llaneras MR, Nance ML, Streicher JT, et al. Large-animal model of ischemic mitral regurgitation. *Ann Thorac Surg* 1994;57:432-439
 25. Sutton MS, Pfeffer MA, Plappert T, et al. Quantitative 2-dimensional echocardiographic measurements are major predictors of adverse cardiovascular events after acute myocardial infarction: The protective effects of captopril. *Circulation* 1994;89:68-75
 26. Saraste A, Pulkki K, Kallajoki M, Henriksen K, Parvinen M, Voipio-Pulkki LM. Apoptosis in human acute myocardial infarction. *Circulation* 1997;95:320-323
 27. Beyersdorf F, Doenst T, Athanasuleas C, Suma H, Buckberg. The beating open heart for rebuilding ventricular geometry during surgical anterior restoration. *Semin Thorac Cardiovasc Surg* 2001;13:42-51
 28. Menicanti L, DiDonato M, Castelvechio S, et al., and the RESTORE group. Functional ischemic mitral regurgitation in anterior ventricular remodeling: Results of surgical ventricular restoration with and without mitral repair. *Heart Fail Rev* 2004;9:317-327
 29. Kelley ST, Malekan R, Gorman JH, et al. Restraining infarct expansion preserves left ventricular geometry and function after acute anteroapical infarction. *Circulation* 1999;99:135-142
 30. Moainie SL, Guy S, Gorman JH, et al. Infarct restraint attenuates remodeling and reduces chronic ischemic mitral regurgitation after postero-lateral infarction. *Ann Thorac Surg* 2002;74:444-449
 31. Acker MA, Bolling SF, Mann DL, et al. Mitral valve surgery in heart failure: Results of the Acorn Corcap randomized trial. American Association for Thoracic Surgery, 86th Annual Meeting, Toronto, April 2005.
 32. Mann DL, Acker MA, Jessup M, Sabbah HN, Starling RC. Clinical evaluation of Corcap cardiac support device in patients with dilated cardiomyopathy. American Heart Association Scientific Sessions, New Orleans, November 2004.
 33. Pilla JJ, Blom AS, Brockman DJ, et al. Ventricular constraint using the acorn cardiac support device reduces myocardial akinetic area in an ovine model of acute infarction. *Circulation* 2002;106(12 Suppl.1):I207-I211

34. Sabbah HN, Sharov VG, Gupta RC, et al. Reversal of chronic molecular and cellular abnormalities due to heart failure by passive mechanical ventricular containment. *Circ Res* 2003;93:1095-1101
35. Harrington KB, Rodriguez F, Cheng A, et al. Direct measurement of transmural laminar architecture in the anterolateral wall of the ovine left ventricle: New implications for wall thickening mechanics. *Am J Physiol Heart Circulat Physiol* 2005;288:H1324-H1330

Meeting discussion

DR. PRAVIN SHAH (Newport Beach, California, USA): I compliment you on the elegance of your study. Could you tell us about the time course of the shear strain in the remote region? Did that develop as quickly as the infarct was created? Did you examine the time course itself?

DR. ALLEN CHENG (Stanford, California, USA): Yes. Actually we have two studies, one acute and one chronic. In the acute study we looked at the shear strain pattern 1 minute after ischemia is induced, and found that the shear strain perturbation occurred only adjacent to the infarcted area - we have not seen any shear strain pattern at a remote site. We then looked at the shear strain pattern again at one week - it occurred adjacent to the infarct, but we also start to see a pattern of shear

strain at a remote site, but it is not yet significant. But at eight weeks the shear strain pattern becomes very significant at remote sites.

DR. THOMAS JOUDINAUD (Missoula, Montana, USA): We have performed a similar study in which we induced a posterior infarct by percutaneous injection of pure ethanol. Then, at eight weeks we used a molecular biology approach to monitor endothelial nitric oxide synthase (eNOS) production. This enzyme seemed to be related with stretch, and in seven different areas of the heart - anterior, posterior, lateral wall of both ventricles - we found an upregulation of eNOS. This increased nitric oxide production seemed to correspond to the increased stretch in your report.

DR. CHENG: Thank you for the comment.

DR. DANIEL LOISANCE (Creteil, France): You seem to have perfect control of your model and of the technology. Are you planning to place some crystal markers on the papillary muscles or on the valve itself?

DR. CHENG: Yes, we have another study planned in which we will place many radiopaque markers on the leaflet itself. In this way we can build a finite element model of the leaflet, but we may also consider putting radiopaque markers on the papillary muscle.